Open Research Online

Mass wasting triggered by seasonal CO$_2$ sublimation under Martian atmospheric conditions: Laboratory experiments

Journal Item

For guidance on citations see FAQs.

Version: Version of Record

oro.open.ac.uk

Mass wasting triggered by seasonal CO2 sublimation under Martian atmospheric conditions: Laboratory experiments

Matthew E. Sylvest[1] (iD), Susan J. Conway[2,3] (iD), Manish R. Patel[2,4] (iD), John C. Dixon[1] (iD), and Adam Barnes[5] (iD)

[1]Arkansas Center for Space and Planetary Sciences, University of Arkansas, Fayetteville, Arkansas, USA, [2]School of Physical Sciences, Open University, Milton Keynes, UK, [3]Laboratoire de Planétologie et Géodynamique de Nantes-UMR CNRS 6112, Nantes, France, [4]Space Science and Technology Department, STFC Rutherford Appleton Laboratory, Oxfordshire, UK, [5]Center for Advanced Spatial Technologies, University of Arkansas, Fayetteville, Arkansas, USA

Abstract Sublimation is a recognized process by which planetary landscapes can be modified. However, interpretation of whether sublimation is involved in downslope movements on Mars and other bodies is restricted by a lack of empirical data to constrain this mechanism of sediment transport and its influence on landform morphology. Here we present the first set of laboratory experiments under Martian atmospheric conditions which demonstrate that the sublimation of CO_2 ice from within the sediment body can trigger failure of unconsolidated, regolith slopes and can measurably alter the landscape. Previous theoretical studies required CO_2 slab ice for movements, but we find that only frost is required. Hence, sediment transport by CO_2 sublimation could be more widely applicable (in space and time) on Mars than previously thought. This supports recent work suggesting CO_2 sublimation could be responsible for recent modification in Martian gullies.

1. Introduction

Sublimation is a recognized planetary process [*Mangold*, 2011], primarily identified with pitting or uneven lowering of a surface. Sublimation has been implicated as one of several potential mechanisms controlling hillslope processes on Mars, notably recent erosion and deposition in kilometer scale gullies (Figure 1) [*Dundas et al.*, 2015]. Gully-like features are also reported on Vesta [*Krohn et al.*, 2014; *Scully et al.*, 2015] and are seen on the Moon [*Bart*, 2007].

For recent changes in gullies on Mars and Vesta, alternate processes include formation by flowing water and/or brine [*Malin and Edgett*, 2000; *Scully et al.*, 2015]. These "wet" hypotheses are based on the plan view and 3-D morphology of the features, which are consistent with observations of terrestrial analogues, e.g., wet debris flow gullies [*Reiss et al.*, 2011] or seeping flows on Earth [*Kreslavsky and Head*, 2009]. However, there are no terrestrial analogues for the action of sublimation in a hillslope context, which hampers the assessment of whether observations are also consistent with formation by sublimation. The overarching motivation behind this study is therefore to provide experimental data in order to test the ability of sublimation to produce hillslope features and to start to constrain the observables required to identify its action. We focus our study on the seasonal (local spring) sublimation of CO_2 on Mars for two reasons. First, Mars has a seasonal CO_2 condensation-sublimation cycle that is closely linked to many active surface features observed in orbital images [*Kieffer et al.*, 2006; *Gardin et al.*, 2010; *Hansen et al.*, 2011], suggesting a possible causal relationship. And second, because ongoing observations and studies of Martian hillslope features are more numerous and detailed than those for the other bodies cited above.

The only other experiments to date involving mass transport by CO_2 sublimation are field experiments which have explored the morphological effect of levitating blocks of CO_2 ice moving down slip faces of sand dunes [*Diniega et al.*, 2013]. These experiments were focused on reproducing some of the key features of the so-called linear gullies, which are only observed on the surface of large, dark sand dunes in the southern hemisphere of Mars.

Two numerical models have been used to assess the efficacy of downslope transport driven by CO_2 slab ice sublimation on Mars. *Cedillo-Flores et al.* [2011] simulated the fluidization of sediment deposited over a
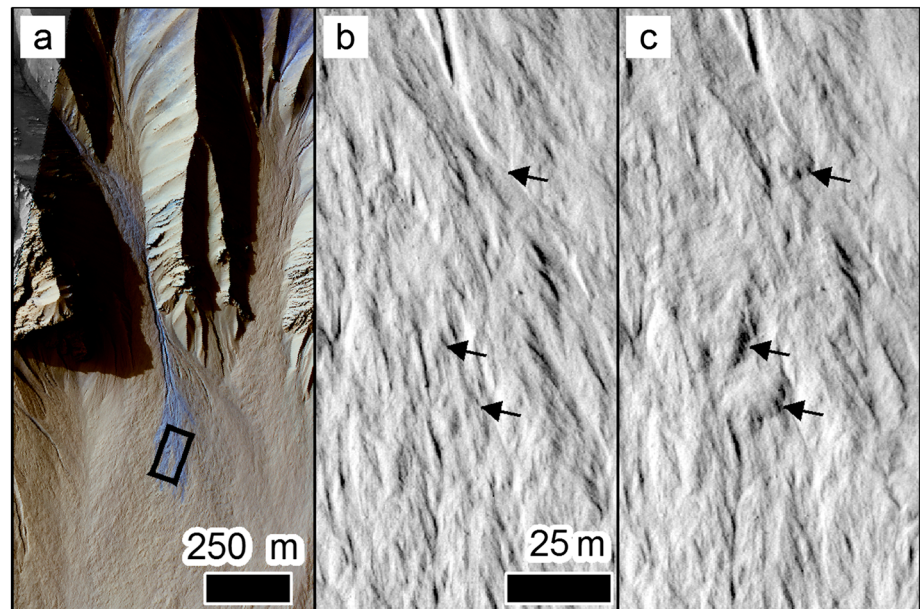
Figure 1. Features thought to be caused by sublimation on Mars. (a) High-Resolution Imaging Science Experiment (HiRISE) image ESP_020661_1440of Martian gullies in Gasa crater. Black box indicates location of Figures 1b and 1c. (b and c) New gully deposits form in winter when CO_2 is present [*Dundas et al.*, 2012; *Vincendon*, 2015] (ESP_012024_1440 and ESP_020661_1440). Image credits: NASA/JPL-Caltech/University of Arizona.

sublimating slab of CO_2 ice. Assuming 0.3–100 mm thick layers of sand (100 μm) and dust (3 μm), they calculated whether the sublimation rate of the underlying CO_2 would be sufficient to mobilize the sediment on a 25° bed, located at 75°N/S. They found sand was always mobilized, while only dust layers <100 mm thick could be mobilized. *Pilorget and Forget* [2016] modeled the mobilization of dry sediment trapped between CO_2 slab ice and an overlying water ice-cemented permafrost. This model was optimized for the "linear" gullies on the Russell crater megadune at 55°S, exploring slope angles between 10 and 30°. They used a climate model to predict that movements generated this way should be possible anywhere poleward of 60°S and on pole-facing slopes poleward of 25°S.

Despite these previous studies being focused on slab ice, there is a lack of observational evidence in support of slab ice occurring equatorward of ~65° [*Kieffer et al.*, 2006]. Also, slab ice requires a long period of time below the condensation temperature in order to develop. CO_2 is known to occur more widely (both spatially and temporally) as surface frost [*Vincendon*, 2015], and this form of CO_2 ice has been observed in regions with recent gully modifications. Therefore, in order to assess the ability of more ubiquitous surface frost to trigger downslope movements, we condensed CO_2 frost directly on the regolith. We performed four experimental runs and one control run.

2. Approach

The three principal requirements of our approach were to (1) condense CO_2 on/into a regolith slope, without introducing water or other ices; (2) sublimate the CO_2 at Martian atmospheric temperature and pressure by means of radiant heating; and (3) record resulting regolith activity for visual and photogrammetric analysis. Use of close-range photogrammetric techniques allowed us to determine slope angles, as well as displacement volumes and rates. Simulation of the Martian environment was achieved in the Mars Chamber at the Open University, Milton Keynes, UK (Figure S1 in the supporting information) [*Conway et al.*, 2011a]. Full details of our approach are in the supporting information, and we provide a brief summary below.

The regolith was contained within a 30 cm long, cooled, copper test section (Figures S2 and S3). The scale of the test section was limited by the time required to cool the sediment body and by the field of view of the video cameras used to record the experiments and produce the digital elevation models (DEM) through stereo photogrammetry. Along with atmospheric temperature and pressure, temperatures within the slope

were logged at multiple depths along the centerline, near the midpoint, and just below the slope crest (Figure S2). A shape movement detection algorithm was also applied to each movie pair, providing a heuristic measure of relative slope surface activity levels.

As a first test of the ability of CO_2 sublimation to trigger slope failure, the regolith was formed into a stable slope near the angle of repose (22–33°), the most favorable condition for slope failure. This configuration was used to ensure that even the smallest disturbance resulted in a detectable motion or failure. The regolith was then cooled to below the freezing point of CO_2 (−112°C) in a dry nitrogen atmosphere (~350 mbar) to ensure the absence of water vapor. Gaseous CO_2 was introduced above the regolith, while continuing to cool, in order to condense CO_2 on and/or within the regolith. The pressure was then lowered in the chamber to the target pressure of ~5–6 mbar consistent with Mars [*Hess et al.*, 1980]. Finally, the surface was illuminated by a heat lamp for at least ~90 min, or until all the recorded temperatures were above −120°C (CO_2 sublimation point at ~5 mbar). The near-surface temperature ranged from –123°C to 9°C over the course of the sublimation process. We calculate that the maximum heat flux at the bare regolith surface as ~350 W/m^2 (details in the supporting information), which is comparable with Viking lander insolation data [*Landis and Appelbaum*, 1990].

3. Results

All four of the experiments resulted in the downslope transport of material induced by CO_2 sublimation. No activity was observed in the control run. In this section, we first describe the nature and timing of the activity and then present the results from the time series elevation models.

3.1. Nature and Timing of Activity

Runs 1, 3, and 4 showed very similar behavior, while run 2 exhibited a number of notable differences. In all experiments, before sublimation began, a visible layer of frost covered the lower one quarter to one half of the slope, concentrating along the test section walls, and particularly at the foot of the slope, where the sediment-depth is ~2 cm (Figures 2a and S4). The first detectable movements in each run were shifting grains of CO_2 frost, which had no effect on the underlying regolith surface. Mass wasting of regolith started within the first 15 min of each run, except for run 2, which became active ~40 min into the run (Figure 3a). These initial failures, up to several centimeters wide, started 4–10 cm downslope of the crest and extended to the base of the slope, where they formed depositional lobes (Figures 2 and 4 and Movie S1). In runs 1, 3, and 4, slope activity peaked within the first 25 min, while run 2 peaked after 60 min (Figure 3). For all runs, activity continued sporadically after the initial peak (Figure 3) and with continued slope failures, grew to the full slope width (Figure 2). For runs 1, 3, and 4, activity extended up to the slope crest (Figures 2 and 4). Slope failures were in the form of granular flows, which initiated below the surface of the slope, proximal to, but never underneath, visible, surface frost. Flows did not appear to disturb surface frost accumulations, generally following lateral contours, and either overran or stopped at the edge of downslope accumulations. Where deposits did cover visible surface frost, the new, overlying surface deposit became pitted by sublimation, occasionally so vigorously agitated as to resemble boiling (Movie S2).

Warming of the test section top edges during the second half of each run caused accumulations of CO_2 ice to fall onto the slope. None of these events resulted in significant sediment transport. Some later slope failures were characterized by an initial slip, followed by a slow slumping or sliding of the material deposited by earlier movements in the lower half of the slope. These slumps occurred where visible frost was observed at the start of each run. This slumping behavior is particularly noticeable in accelerated video replay (Movie S3).

Run 2 differences included (i) at the start of the run surface frost was confined to within bottom-most 3 cm of the slope, (ii) the initial failure occurred at ~40 min into the run, with the earliest movement of this failure being some tumbling grains at the midpoint of the slope, and (iii) the failures were confined to the lower half of the test section and never propagated to the crest of the slope (Figure S5). However, the granular flow nature of the run 2 slope failures was consistent with the other runs.

### 3.2. Evolution of Volumes and Slope Angles

As described in the supporting information, for each 10 min interval, we calculated the volume eroded and deposited by the flows, which implicitly includes the volume of the CO_2 sublimated during the experiment.
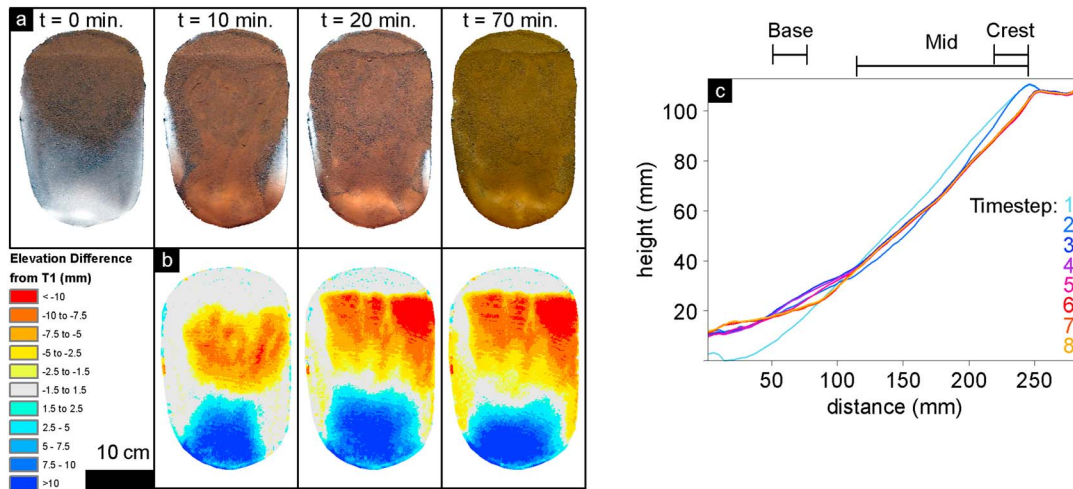
Figure 2. Evolution of the surface during experiment run 3. (a) Orthophotos showing visible appearance of the surface at $t = 0$, 10, 20, and 70 min elapsed sublimation. White coloration is CO_2 surface frost. (b) Topographic change from $t = 0$ to $t = 10$, 20, and 70 min, where red is erosion and blue is deposition. The scale for all images is the same, and the top of every image corresponds to the highest elevation of the test section. (c) Evolution of the topographic long profiles for each time step of run 3. The regions used to measure the slope angles reported in Table 1 are indicated at the top.

Volume transport rates calculated from the DEMs (e.g., Figure 2b) were consistent with the timing of surface activity in Figure 3a. During the first 10–20 min of runs 1, 3, and 4, most erosion takes place in the middle of the slope, initiating 2–3 cm below the crest. As each run progresses, most of the upper slope erodes, causing the crest to retreat (Figure 2b and Movie S4). This phase of activity establishes the maximum areal extent of deposition and encompasses the peak erosion rate shown in Figure 3b. Later slope failures, although infrequent and sporadic, continued to transport regolith downslope; however, these were a minor contribution to the overall volume transported (Figures 2b and 3b). For run 2, activity started later, began midslope (concentrated at the edges), never extended up to the slope crest (Figure S6b) and volumes of sediment were moved sporadically throughout (Figure 3). The recorded change in elevation due to erosion was 0.02–1.1 cm, and 0.02–1.3 cm of deposition for all runs.

The total erosion volume ranges between 122 and 173 cm^3 for runs 1, 3, and 4, ~3.4% of the initial regolith volume, on average (Table 1). For run 2, the erosion volume is 69 cm^3; ~1.6% of the initial regolith volume.
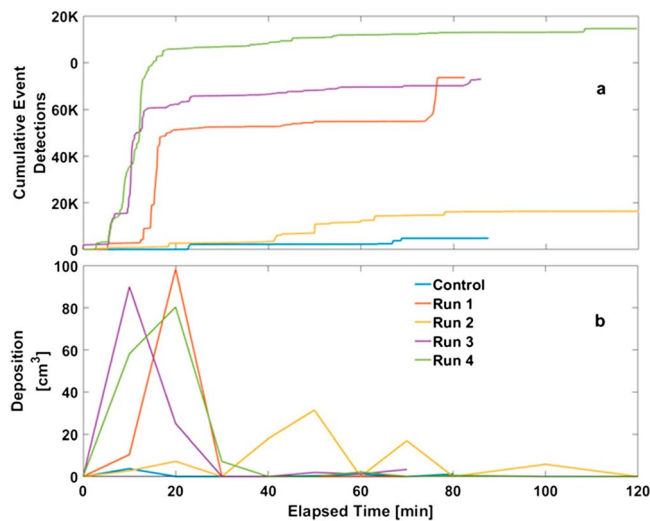
Figure 3. Sublimation induced "activity" and deposition rate over time for each experimental run. (a) Cumulative plot of "events" detected via motion detection against time. (b) Variation of deposition rate over time for each run, calculated by differencing elevation models at ~10 min time steps.

Table 1. Summary of Experimental Results[a]

	Control	Run 1	Run 2	Run 3	Run 4
Total erosion (cm^3)	27.2	122.6	68.6	173.3	144.5
Total deposition (cm^3)	3.8	85.4	46.2	101.5	127.0
Frost volume (cm^3)	n/a	37.2	22.4	71.8	17.5
Erosion per volume frost	n/a	3.3	3.10	2.4	8.3
Volume uncertainty	2.2%	3.0%	1.6%	3.6%	3.5%
Crest Slope Angles					
Initial angle	25.4°	32.6°	25.9°	25.3°	21.6°
Final angle	25.2°	27.8°	26.4°	31.6°	31.1°
Angle change	−0.2°	−4.7°	0.5°	6.3°	9.5°
Midslope Angles					
Initial angle	27.8°	28.3°	27.2°	29.7°	25.7°
Final angle	27.8°	24.2°	29.1°	27.4°	22.1°
Angle change	0.0°	−4.1°	1.9°	−2.3°	−3.55°
Base Slope Angles					
Initial angle	29.7°	18.3°	26.2°	22.7°	23.2°
Final angle	29.8°	13.7°	10.1°	8.30°	5.87°
Angle change	0.1°	−4.6°	−16.1°	−14.4°	−17.3°
Angle uncertainty	1.1%	2.0%	1.0%	3.0%	1.1%
Average initial slope temperature (°C)	−150.4	−142.3	−143.5	−143.5	−143.6
Average Initial basal slope temperature (°C)	−168.0	−161.8	−171.2	−167.5	−167.1
Sublimation duration (min)	88	87	109	86	121

[a]Regolith volume for all runs was 4330 cm^3.

The deposition volume is between 85 and 127 cm^3 (~2.4% of the initial volume on average) for runs 1, 3, and 4, and ~1.1% for run 2. Erosion generally exceeded deposition, which we interpret as being due to the removal of the condensed CO_2 ice. As direct measurement of the CO_2 ice volume was infeasible, the difference between erosion and deposition volumes was used to estimate a minimum solid CO_2 volume (Table 1). For all runs, sublimation of 1 cm^3 of CO_2 ice resulted in the erosion of 2.4–8.3 cm^3 of regolith (Table 1).

We measured an average reduction of slope along the centerline of ~4.1° for runs 1, 3, and 4 (Table 1), ~90% of that change occurring within the first 20 min of the run (Figure 2c). These failures initiated on slope angles between 22° and 32° (crest angles in Table 1). Over the course of the experiment, slope angles were retained at the crest of the profile but declined in both the midslope and base slope areas (Figures 2c and S6). For run 2, late activity was restricted to the midportion of the slope, and this failure initiated at an angle of 25.6° (Figure S5). For the later slumps in runs 1, 3, and 4, initiation at angles as low as 13° was observed (Figure S5a). These late slumps account for the majority of the volume difference seen in Figure 2, between $t = 20$ min and $t = 70$ min, in the bottom half of the test section.

4. Discussion

4.1. Physical Processes and Comparison to Previous Models

From our observations, we hypothesize that the porous nature of the regolith allows gas to infiltrate and freeze in the cold subsurface during the condensation procedure. Then, during the rapid production of gas during sublimation, the regolith pores restrict gas escape, allowing pore pressure to increase to the point of slope failure.

This mechanism triggered failures at angles less than the static angle of repose ~38° [*Sullivan et al.*, 2011], but nearer the dynamic angle of repose ~29° [*Hofmann*, 2014], which suggests that sublimation provides the initial destabilization and is followed by a nonfluidized granular flow. However, further work is required in order to properly substantiate this observation. Later failures, initiating in areas originally covered with frost, were triggered at slope angles significantly below the dynamic angle of repose (down to 13°). We propose that this is a result of the sublimation of an underlying layer of CO_2 ice both triggering and fluidizing the flow. This second mechanism is consistent with the model presented by *Cedillo-Flores et al.* [2011], in which a solid CO_2 slab overlain with up to 10 cm of aeolian-emplaced regolith (sand or dust), a highly unstable configuration, subsequently fluidizes.

In this first phase of experimentation, we did not intend to quantify the effects of the reduced gravity of Mars, relative to the Earth. However, theoretical considerations predict that the escaping gas velocity required to fluidize particles would be lower on Mars than on Earth. This suggests that the slope failures we observed would be more easily triggered and more erosive on Mars; thus, the results presented here may be conservative with respect to this sublimation process on Mars.

Failures were initiated in areas devoid of visible frost. This is significant, as the visible/spectral presence of CO_2 frost has been associated with present-day gully-activity on Mars [*Hugenholtz*, 2008; *Vincendon*, 2015], including the extension of "thin" deposits [*Malin et al.*, 2006; *McEwen et al.*, 2007] and particularly the development of new channels (Figures 1a–1c) and new, meter thick deposits [*Dundas et al.*, 2015]. We hypothesize that the cold temperature and high albedo of the surface frost accumulations in our experiments inhibit sublimation underneath the frost and if thick enough may indurate the surface. Sediment movement triggered by this type of CO_2 sublimation on Mars may therefore be most likely to initiate adjacent to visible frost, or after visible frost has disappeared from the surface. As a result of these observations, we suggest that future experiments should carefully examine the partitioning between surface and subsurface frost.

4.2. Implications for Interpreting Slope Processes on Mars

While the spatial scale of our experiments does not allow direct comparison with full-scale surface features, like gullies, our results do establish the potential for CO_2 sublimation to trigger mass wasting of dry, unconsolidated material on sloping surfaces under Martian environmental conditions. This supports the assertions of previous research that CO_2 sublimation could be responsible for recent movements detected in gullies and seasonal sediment flows observed on Martian dunes [*Diniega et al.*, 2010; *Reiss et al.*, 2010; *Dundas et al.*, 2012; *Pasquon et al.*, 2016]. As noted earlier, the particular mechanism explored here only applies to movements which occur in the absence of slab ice. The movement of 1–2 m scale boulders down the gully channels in the presence of visible CO_2 frost observed by *Dundas et al.* [2015] is also unlikely to be caused by the mechanism discussed here but warrants further experimental investigation. The latitudinal distribution of recurring slope lineae [*McEwen et al.*, 2014] is not consistent with the seasonal extent of CO_2 frost [*Vincendon*, 2015; *Piqueux et al.*, 2016]; hence, this mechanism could not universally be applied to these features. The distribution of slope streaks [*Sullivan et al.*, 2001; *Schorghofer et al.*, 2002] has recently been found to correlate with the nighttime occurrence of CO_2 frost in areas with high dust and low thermal inertia, at middle to equatorial latitudes [*Piqueux et al.*, 2016]. *Piqueux et al.* [2016] estimate that up to 350 μm of frost could be deposited onto the surface at night and that deposition of frost into the subsurface would require subsurface cold traps. While our experiments were focused on seasonal frost, our observations support the need for subsurface frost deposits to initiate sediment movements.

Our observations suggest that this is a slope-limited process, similar to other gravity driven mass wasting processes, such as wet debris flows and landslides [*Lague and Davy*, 2003; *DiBiase et al.*, 2012]. We emphasize that we do not expect angular limits found in our experiments to apply on Mars due to the difference in gravitational acceleration; however, this observation shows that the CO_2 sublimation process is feasible beyond the domain of gravity triggered granular flows. *Brusnikin et al.* [2016] reported a slope limit of 18–20°, below which they found very few initiations of granular flows, and suggested these flows are limited by the dynamic angle of friction. This is consistent with our finding that granular flows not fluidized by sublimating ice initiate at angles >20°, in our experiments. Because slope angle is often a key factor used to distinguish between different geomorphic processes [*Lanza et al.*, 2010; *Conway et al.*, 2011b], this is an important area which warrants further investigation to further constrain the slope limits of this type of sublimation-triggered slope failure.

Our experimental results show that CO_2 sublimation can trigger movement without the ice being in the form of a slab. Thus, CO_2 sublimation could be a more widely active agent of surface alteration than previously assumed, particularly in light of the discovery of an equatorial, diurnal CO_2 cycle [*Piqueux et al.*, 2016].

Gully modifications have been reported at midlatitudes on Mars, where seasonal surface frost can be on the order of millimeter to centimeters thick [*Vincendon*, 2015], and volumes of displaced sediment have been estimated at tens to hundreds of cubic meters [*Dundas et al.*, 2015]. Based on our calculated rate of sediment displacement per CO_2 ice volume (Table 1 and supporting information), the aforementioned thickness and displacement volume ranges require areas of frost-laden sediment hundreds to tens of thousands of square

meters. This is consistent with the observation that source areas commonly display "minor morphological effects" [*Dundas et al.*, 2015].

4.3. Wider Implications

Understanding how CO_2 interacts with geological materials under Martian conditions is fundamental to our interpretation of current geomorphological activity, atmospheric evolution, and the history of water on Mars. Forms such as gullies, for example, are found over much of the surface of Mars [*Harrison et al.*, 2015] and were initially interpreted as evidence for the action of substantial quantities of liquid water [*Malin and Edgett*, 2000]. The possibility of CO_2-induced gully modification means water may not always be necessary to form such features [*Dundas et al.*, 2015]. A deeper understanding of the mechanism of hillslope modification by sublimation is required before we can interpret present-day changes, much less attempt to interpret landscape evolution over the Amazonian period.

In a wider context, sublimation affects the surfaces of other terrestrial planets. Hence, understanding sublimation as a sediment transport mechanism has implications beyond Mars and will guide interpretation of data coming from a wide range of current and future planetary space missions.

5. Conclusions

We have demonstrated for the first time, in the laboratory, that sublimation of condensed CO_2 frost, under Martian atmospheric conditions, can trigger mass wasting of unconsolidated regolith. These results provide one possible explanation for recent modifications observed in gullies, without the need for liquid water. The observed slope failures are dry granular flows, apparently triggered by the sublimation of CO_2 ice condensed in the regolith pore space. Fluidization of regolith over subsurface frost may allow for sediment transport at angles below the dynamic angle of repose. The CO_2 frost sublimation trigger mechanism may have broader spatial and temporal applicability on Mars than CO_2 slab mechanisms. Although not directly simulated in these experiments, our results suggest sublimating diurnal CO_2 frost may help explain the behavior and distribution of enigmatic Martian slope streaks, recently found to correlate with diurnal CO_2 frost locations.

These experiments represent an important first step in understanding the role of sublimation as a landscape-forming process in the solar system and underline the urgent need for further laboratory work to constrain the limits (slope angle, grain size, etc.) of CO_2-driven processes to support meaningful comparisons between observed morphologies and formation processes.

References

Bart, G. D. (2007), Comparison of small lunar landslides and Martian gullies, *Icarus*, *187*(2), 417–421, doi:10.1016/j.icarus.2006.11.004.

Brusnikin, E. S., M. A. Kreslavsky, A. E. Zubarev, V. D. Patratiy, S. S. Krasilnikov, J. W. Head, and I. P. Karachevtseva (2016), Topographic measurements of slope streaks on Mars, *Icarus*, *278*, 52–61, doi:10.1016/j.icarus.2016.06.005.

Cedillo-Flores, Y., A. H. Treiman, J. Lasue, and S. M. Clifford (2011), CO_2 gas fluidization in the initiation and formation of Martian polar gullies, *Geophys. Res. Lett.*, *38*, L21202, doi:10.1029/2011GL049403.

Conway, S. J., M. R. Balme, M. P. Lamb, M. C. Towner, and J. B. Murray (2011a), Enhanced runout and erosion by overland flow under subfreezing and low pressure conditions: Experiments and application to Mars, *Icarus*, *211*(1), 443–457, doi:10.1016/j.icarus.2010.08.026.

Conway, S. J., M. R. Balme, J. B. Murray, M. C. Towner, C. H. Okubo, and P. M. Grindrod (2011b), The indication of Martian gully formation processes by slope–area analysis, *Geol. Soc. Lond. Spec. Publ.*, *356*(1), 171–201, doi:10.1144/SP356.10.

DiBiase, R. A., A. M. Heimsath, and K. X. Whipple (2012), Hillslope response to tectonic forcing in threshold landscapes, *Earth Surf. Processes Landforms*, *37*(8), 855–865, doi:10.1002/esp.3205.

Diniega, S., S. Byrne, N. T. Bridges, C. M. Dundas, and A. S. McEwen (2010), Seasonality of present-day Martian dune-gully activity, *Geology*, *38*(11), 1047–1050, doi:10.1130/G31287.1.

Diniega, S., C. J. Hansen, J. N. McElwaine, C. H. Hugenholtz, C. M. Dundas, A. S. McEwen, and M. C. Bourke (2013), A new dry hypothesis for the formation of Martian linear gullies, *Icarus*, *225*(1), 526–537, doi:10.1016/j.icarus.2013.04.006.

Dundas, C. M., S. Diniega, C. J. Hansen, S. Byrne, and A. S. McEwen (2012), Seasonal activity and morphological changes in Martian gullies, *Icarus*, *220*(1), 124–143, doi:10.1016/j.icarus.2012.04.005.

Dundas, C. M., S. Diniega, and A. S. McEwen (2015), Long-term monitoring of Martian gully formation and evolution with MRO/HiRISE, *Icarus*, *251*, 244–263, doi:10.1016/j.icarus.2014.05.013.

Gardin, E., P. Allemand, C. Quantin, and P. Thollot (2010), Defrosting, dark flow features, and dune activity on Mars: Example in Russell crater, *J. Geophys. Res.*, *115*, E06016, doi:10.1029/2009JE003515.

Hansen, C. J., et al. (2011), Seasonal erosion and restoration of Mars' northern polar dunes, *Science 331*, 575, doi:10.1126/science.1197636.

Harrison, T. N., G. R. Osinski, L. L. Tornabene, and E. Jones (2015), Global documentation of gullies with the Mars Reconnaissance Orbiter Context Camera and implications for their formation, *Icarus*, *252*, 236–254, doi:10.1016/j.icarus.2015.01.022.

Hess, S. L., J. A. Ryan, J. E. Tillman, R. M. Henry, and C. B. Leovy (1980), The annual cycle of pressure on Mars measured by Viking Landers 1 and 2, *Geophys. Res. Lett.*, *7*(3), 197–200, doi:10.1029/GL007i003p00197.

Hofmann, M. (2014), Dynamics of granular material on small bodies, Technischen Universität Braunschweig.

Hugenholtz, C. H. (2008), Frosted granular flow: A new hypothesis for mass wasting in Martian gullies, *Icarus*, *197*(1), 65–72, doi:10.1016/j.icarus.2008.04.010.

Kieffer, H. H., P. R. Christensen, and T. N. Titus (2006), CO_2 jets formed by sublimation beneath translucent slab ice in Mars' seasonal south polar ice cap, *Nature*, *442*(7104), 793–796, doi:10.1038/nature04945.

Kreslavsky, M. A., and J. W. Head (2009), Slope streaks on Mars: A new "wet" mechanism, *Icarus*, *201*, 517–527.

Krohn, K., R. Jaumann, and K. Otto (2014), Mass movement on Vesta at steep scarps and crater rims, *Icarus*, *244*, 120–132, doi:10.1016/j.icarus.2014.03.013.

Lague, D., and P. Davy (2003), Constraints on the long-term colluvial erosion law by analyzing slope-area relationships at various uplift rates in the Siwaliks Hills (Nepal), *J. Geophys. Res.*, *108*(2), 2129, doi:10.1029/2002JB001893.

Landis, G. A., and J. Appelbaum (1990), Design considerations for Mars photovoltaic power systems, in *Proceedings 21st IEEE Photovoltaic Specialists Conf*, pp. 1263–1270 , IEEE, New York.

Lanza, N. L., G. A. Meyer, C. H. Okubo, H. E. Newsom, and R. C. Wiens (2010), Evidence for debris flow gully formation initiated by shallow subsurface water on Mars, *Icarus*, *205*(1), 103–112, doi:10.1016/j.icarus.2009.04.014.

Malin, M. C., and K. S. Edgett (2000), Evidence for recent groundwater seepage and surface runoff on Mars, *Science*, *288*(5475), 2330–2335, doi:10.1126/science.288.5475.2330.

Malin, M. C., K. S. Edgett, L. V. Posiolova, S. M. McColley, and E. Z. N. Dobrea (2006), Present-day impact cratering rate and contemporary gully activity on Mars, *Science*, *314*(5805), 1573–1577.

Mangold, N. (2011), Ice sublimation as a geomorphic process: A planetary perspective, *Geomorphology*, *126*(1–2), 1–17, doi:10.1016/j.geomorph.2010.11.009.

McEwen, A. S., et al. (2007), A closer look at water-related geologic activity on Mars, *Science*, *317*(5845), 1706–1709, doi:10.1126/science.1143987.

McEwen, A. S., C. M. Dundas, S. S. Mattson, A. D. Toigo, L. Ojha, J. J. Wray, M. Chojnacki, S. Byrne, S. L. Murchie, and N. Thomas (2014), Recurring slope lineae in equatorial regions of Mars, *Nat. Geosci.*, *7*(1), 53–58, doi:10.1038/ngeo2014.

Pasquon, K., J. Gargani, M. Massé, and S. J. Conway (2016), Present-day formation and seasonal evolution of linear dune gullies on Mars, *Icarus*, *274*, 195–210, doi:10.1016/j.icarus.2016.03.024.

Pilorget, C., and F. Forget (2016), Formation of gullies on Mars by debris flows triggered by CO_2 sublimation, *Nat. Geosci.*, *9*, 65–69.

Piqueux, S., A. Kleinböhl, P. O. Hayne, N. G. Heavens, D. M. Kass, D. J. McCleese, J. T. Schofield, and J. H. Shirley (2016), Discovery of a widespread low-latitude diurnal CO_2 frost cycle on Mars: Low-latitude CO_2 frost on Mars, *J. Geophys. Res. Planets*, *121*, 1174–1189, doi:10.1002/2016JE005034.

Reiss, D., G. Erkeling, K. E. Bauch, and H. Hiesinger (2010), Evidence for present day gully activity on the Russell crater dune field, Mars, *Geophys. Res. Lett.*, *37*, L06203, doi:10.1029/2009gl042192.

Reiss, D., et al. (2011), Terrestrial gullies and debris-flow tracks on Svalbard as planetary analogs for Mars, *Geol. Soc. Am. Spec. Pap.*, *483*, 165–175, doi:10.1130/2011.2483(11).

Schorghofer, N., O. Aharonson, and S. Khatiwala (2002), Slope streaks on Mars: Correlations with surface properties and the potential role of water, *Geophys. Res. Lett.*, *29*(23), 2126, doi:10.1029/2002GL015889.

Scully, J. E. C., C. T. Russell, A. Yin, R. Jaumann, E. Carey, J. Castillo-Rogez, H. Y. McSween, C. A. Raymond, V. Reddy, and L. Le Corre (2015), Geomorphological evidence for transient water flow on Vesta, *Earth Planet. Sci. Lett.*, *411*, 151–163, doi:10.1016/j.epsl.2014.12.004.

Sullivan, R., P. Thomas, J. Veverka, M. Malin, and K. S. Edgett (2001), Mass movement slope streaks imaged by the Mars Orbiter Camera, *J. Geophys. Res.*, *106*(E10), 23,607–23,633, doi:10.1029/2000JE001296.

Sullivan, R., R. Anderson, J. Biesiadecki, T. Bond, and H. Stewart (2011), Cohesions, friction angles, and other physical properties of Martian regolith from Mars Exploration Rover wheel trenches and wheel scuffs, *J. Geophys. Res.*, *116*, E02006, doi:10.1029/2010JE003625.

Vincendon, M. (2015), Identification of Mars gully activity types associated with ice composition, *J. Geophys. Res. Planets*, *120*, 1859–1879, doi:10.1002/2015JE004909.